

# Power Characteristics in Coaxial Mixing: Newtonian and Non-Newtonian Fluids

Stéphane Foucault, Gabriel Ascanio, and Philippe A. Tanguy\*

URPEL, Department of Chemical Engineering, André Aisenstadt Building, Room M-5505, Ecole Polytechnique of Montreal, P. O. Box 6079, Station Centre-ville, Montreal QC H3C 3A7, Canada

The power consumption of a coaxial mixer consisting of a wall-scraping anchor and different dispersion impellers (radial discharge) operating in co- and counterrotating modes has been experimentally characterized in the case of viscous Newtonian and non-Newtonian fluids. It was found that the anchor speed did not affect the power consumption of the dispersion turbines. The power consumption of the anchor was found to increase when the dispersion impellers were used in counterrotating mode and to decrease when they were used in corotating mode. Following the Metzner and Otto approach [*AIChE J.* **1957**, 3 (1), 3–10], new correlations based on the impeller geometry for the generalized Reynolds number and the power number are proposed, and it is shown that a power master curve can be generated for speed ratios larger than 10.

## Introduction

The importance of the mixing quality during a chemical reaction in a batch or continuous process is well recognized. The major design task is the selection of the most appropriate mixing system according to the process specifications. The selection criteria are often based on the mixture quality (homogenization) and the power consumption.<sup>1</sup> The selection of the hydrodynamic conditions for a specific process can be particularly challenging, especially when dealing with time-dependent rheology products. In some cases, the product viscosity, initially close to that of water, can reach several pascal-seconds, thus changing the flow regime and the fluid dynamics in the vessel. It then becomes harder to control the reaction in the tank, especially in poorly agitated zones or the dead zones of the environment.<sup>2,3</sup> Many examples of this particular case can be observed in the field of polymerization and in fermentation processes in which the agitation becomes critical to ensure both good productivity and high selectivity.

The evolution of the fluid rheology can also be caused by the physical changes of the solution microstructure (flocculation, gelation, dispersion, etc.). The final viscosity of the product is often higher than the viscosity of each individual ingredient composing the mixture. Depending on the nature of the products to be dispersed, non-Newtonian properties can also develop (nonlinear viscosity, thixotropic behavior, etc.).

Several innovative strategies have been proposed to control or eliminate segregated regions in stirred vessels, based, for instance, on coaxial mixers, planetary mixers, conical mixers, and dual mixers comprising several impellers rotating at different speeds. Both numerical and experimental work has been carried out to characterize planetary mixers,<sup>4</sup> conical mixers,<sup>5</sup> and several types of coaxial mixers.<sup>6–15</sup> A classical example of a coaxial mixer is the combination of a high-speed turbine and a low-speed anchor scraper. It has been shown that these technologies are capable of adequately

mixing and kneading high-solids-content media such as coating fluids and pastes and of dispersing gas in aerated mixing vessels with a low power consumption, even in the presence of a non-Newtonian rheology. In practice, however, the design of coaxial mixers is based on empirical considerations and industrial experience, and limited knowledge is available for optimizing the system.

Because of the complex arrangement of a coaxial mixer (several different impellers, two agitation speeds, two possible rotation modes), it is quite difficult to characterize the mixing system in terms of the power consumption. Tanguy and Thibault<sup>12,13</sup> determined the power consumption of a new coaxial mixer consisting of a wall-scraping arm (anchor) and a series of rods and a pitched-blade turbine operating in counterrotating mode. They found that the power was a function of the speed ratio of the fast agitator to the slow agitator in both the laminar and turbulent regimes. Their correlations allowed for the prediction of the total power consumption of the system, but they did not allow for the independent evaluation of the influence of each agitator on the total power consumption. Recently, Foucault et al.<sup>15</sup> have shown that the power consumption of radial discharge turbines is not affected by the anchor rotation whether in co- or counterrotating mode. Contrary to these findings, Köhler et al.<sup>14</sup> observed a large influence of the anchor on the power consumption of a central agitator provided with flat paddles in counterrotating mode, for impeller tip speed ratios between 0 and 10. Vanhove et al.<sup>6</sup> studied the power consumption of a double coaxial mixer for the preparation of a silica gel in counterrotating mode. Using two Mixel TTP propellers on the central shaft, they demonstrated that the power consumption of the propellers in the turbulent regime was not affected by the anchor for speed ratios larger than 7.67. All of the above studies clearly indicate that the interaction between the central agitator and the scraping agitator affects the power consumption of each impeller, the degree of which depends on the system geometry and the speed ratio selected. Because the various correlations available were unfortunately developed for specific geometries, it is not

\* To whom correspondence should be addressed. E-mail: philippe.tanguy@polymtl.ca. Tel.: 1-514-340-4040. Fax: 1-514-340-4105.

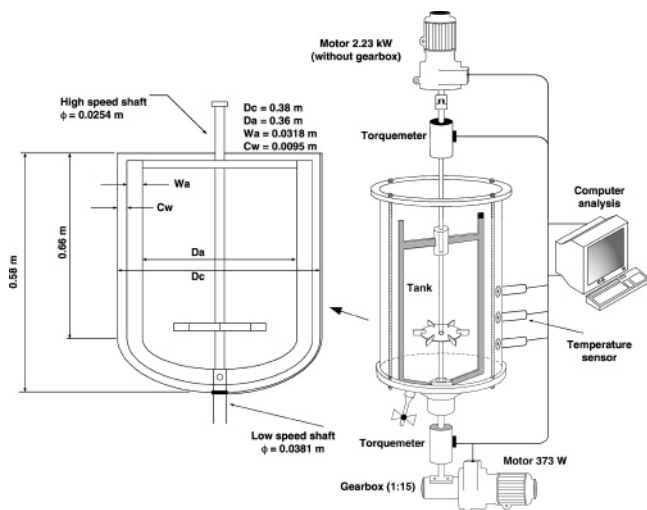


Figure 1. Experimental setup.

Table 1. Laboratory Coaxial Mixer Parameters

parameter	value
tank diameter ( $D_c$ )	0.38 m
turbine diameter ( $D_t$ )	0.2 m
anchor diameter ( $D_a$ )	0.36 m
turbine height (bottom clearance)	$D_t/3$

possible to use them easily to find the total power consumption with other designs.<sup>15</sup>

To overcome this problem, we have developed a laboratory coaxial mixer equipped with two independent drives allowing for the characterization of each agitator. The coaxial mixer consists of an anchor and different dispersion turbines mounted on the same shaft. The main objective of this work is to determine the influence of the power dissipated by each individual impeller on the total power consumption. The study was performed in the laminar and turbulent regimes, and both co- and counterrotating modes were considered.

## Materials and Methods

**Apparatus.** The mixer used for this study and the main geometrical parameters are shown in Figure 1 and Table 1, respectively. The tank is composed in its upper section of a polycarbonate cylinder having a diameter ( $D_c$ ) of 0.38 m, a height ( $H_c$ ) of 0.58 m, and an elliptic dish bottom. The liquid height ( $H_l$ ) of 0.41 m was kept constant throughout the tests, so that the total fluid volume was 46 L.

The coaxial mixer is fitted with two kinds of agitators: a high-speed impeller and a low-speed scraper mounted on two independently actuated coaxial shafts. The high-speed impeller consist of dispersing turbines that can rotate up to 1600 rpm, whereas the other shaft supports a close-clearance anchor rotating at low speed (0 to 100 rpm). The high-speed impellers are mounted in the middle of the tank, generating a radial flow, whereas the low-speed scraper generates mainly a tangential flow. Figure 2a–d shows the high-speed impellers corresponding to various dispersing disk designs, and Figure 2e shows a Rushton turbine.

Two independent motors are used to drive the agitators, and they can be operated in co- and counterrotating modes (see Figure 3). Because the drives are independent, it is possible to rotate only the anchor or to rotate the high-speed impeller while keeping the anchor at rest. In this case, the anchor plays the role of a baffle.

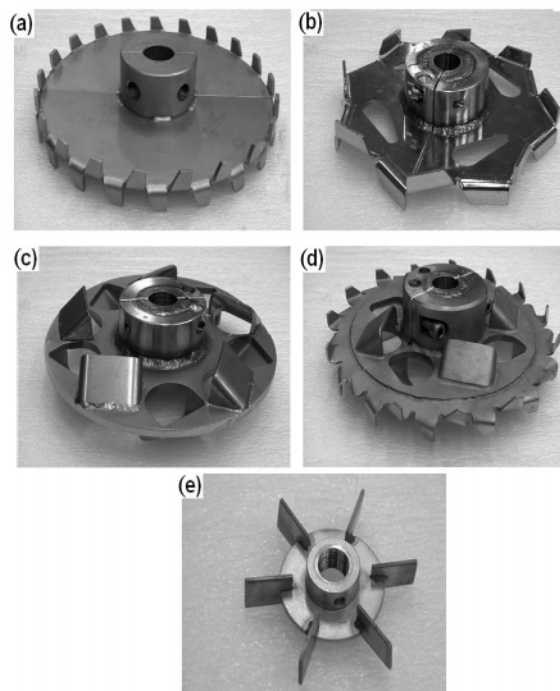


Figure 2. High-speed impellers: (a) Cowles turbine, (b) Deflo turbine, (c) Sevin turbine, (d) hybrid turbine, (e) Rushton turbine.

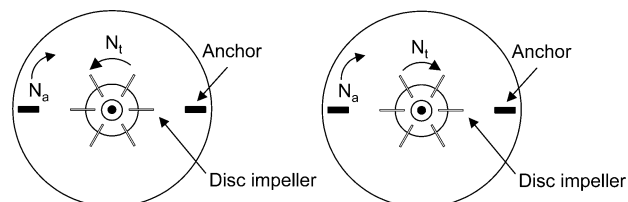


Figure 3. Rotation mode: (a) counterrotation, (b) corotation.

To determine the power dissipated by the different impellers, the motors have been coupled to torque meters having ranges from 0 to 22 N·m for the fast shaft and from 0 to 11 N·m for the slow shaft. In the experiments, the power input was calculated from the induced torque ( $M$ ) and measurements as  $P = \omega M$ , where  $\omega$  is the shaft rotational speed in radians per second. Because the shaft guiding system induces a residual torque due to friction, the resulting torque of friction was measured and subtracted from experimental data, i.e.

$$M_c = M_m - M_r \quad (1)$$

where  $M_c$ ,  $M_m$ , and  $M_r$  are the corrected, measured, and residual torques, respectively (expressed in newton-meters).

**Fluids and Rheology.** Aqueous solutions of corn syrup (80–100 wt %) and carboxymethyl cellulose (CMC, Finnfix 700 and 30000) were chosen as Newtonian and non-Newtonian fluids, respectively. The rheological properties of the solutions were determined at room temperature ( $\sim 23^\circ\text{C}$ ) with a rheometer (AR 2000, TA Instruments) by using a Couette configuration of 30- and 28-mm diameters for the inside and outside cylinders, respectively. The viscosity of the Newtonian fluids ranged from 0.001 to 50 Pa·s, and the density was between 1000 and 1350 kg/m<sup>3</sup>. Because the corn syrup solutions are sensitive to temperature changes, three thermocouples were mounted in the tank to allow the

**Table 2. Properties of the Non-Newtonian Fluids (23 °C)**

solution	$n$	$k$ (Pa·s <sup><math>n</math></sup> )	density (kg/m <sup>3</sup> )	$\dot{\gamma}$ range (s <sup>-1</sup> )
2.5 wt % CMC (Finnfix 700)	0.50	8.3	1010	100–10000
1.5 wt % CMC (Finnfix 30000)	0.22	60	1010	100–10000

temperature evolution to be tracked for each test, so as to correct the viscosity values when necessary. The rheological parameters of the non-Newtonian fluids were found to obey a power law (Table 2). Oscillatory shear tests revealed that the non-Newtonian fluids exhibited a small storage modulus ( $G'$ ) compared to the loss modulus ( $G''$ ). Because the ratio  $G'/G''$  was much smaller than 1, elastic effects were considered to be negligible.

## Results and Discussion

**Power Draw Analysis.** A preliminary power analysis was first carried out by considering the power dissipated by each individual agitator with both Newtonian and non-Newtonian fluids. The results obtained from this part were then compared with the power drawn by the coaxial mixer for different speed ratios and the two rotating modes.

**Single Impeller.** The power consumption of an impeller with Newtonian fluids is usually expressed in terms of the dimensionless power number,  $N_p$ , as a function of the Reynolds number,  $Re$ , without vortex, where  $N_p = P/\rho N^3 D^5$  and  $Re = \rho ND^2/\mu$ . This procedure provides a characteristic power curve that depends only on impeller geometry and can be used to predict power requirements for any given fluid properties, impeller dimensions, and rotational speed. In the laminar regime, it is usual to determine the power constant  $K_p$  defined as follows

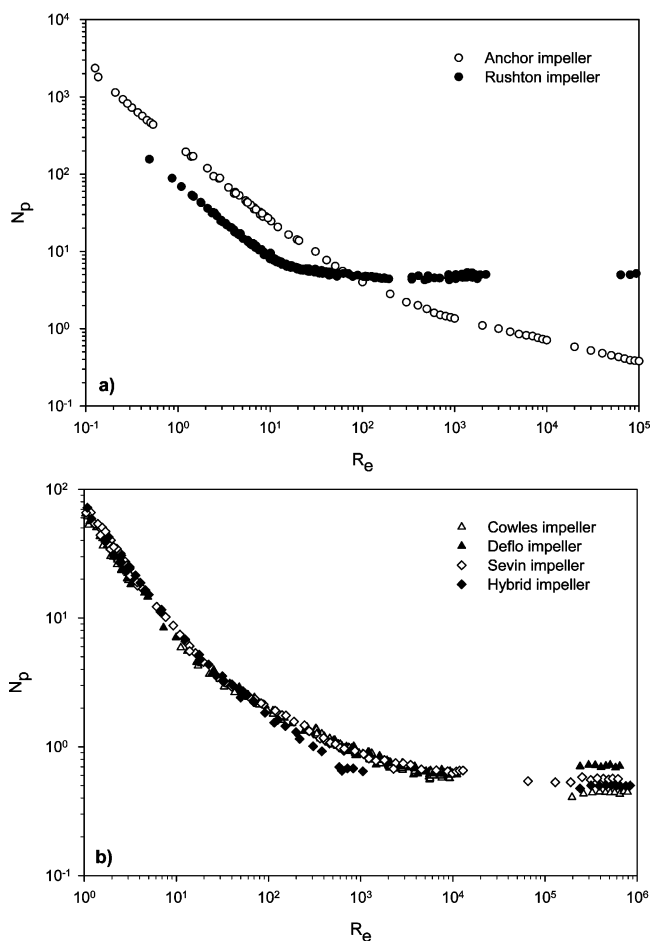
$$K_p = N_p Re \quad (2)$$

For a Newtonian fluid,  $K_p$  is a function of only the impeller geometry.

The characteristic power curve was established for each of the six agitators. The power consumption results served not only to estimate the mechanical energy drawn during the mixing operation, but also to determine the limits among the different flow regimes (laminar, transition, and turbulent).

The characteristic power curves with Newtonian fluids are presented in Figure 4. In agreement with theory, the value of the slope of each curve is equal to  $-1$  in the laminar regime. We note that the anchor agitator operates in the laminar regime for  $Re$  values lower than 100 and the flow becomes transitional for larger values. In the case of the Rushton turbine, the flow is laminar for  $Re$  values lower than 20 and turbulent for  $Re$  values larger than 1000. For the dispersion impellers, the laminar regime corresponds to  $Re$  values lower than 10 and the turbulent regime to  $Re$  values larger than 4500. The corresponding  $K_p$  and  $N_p$  values for the turbulent regime for the six impellers are listed in Table 3. A good agreement is obtained with the literature values.<sup>16–18</sup>

Figure 4 shows that the  $N_p$  value in the turbulent regime does not change with increasing Reynolds number for the dispersion impellers and the Rushton turbine. Because the anchor plays the role of a baffle

**Figure 4.** Newtonian power curve for (a) Rushton and anchor impellers and (b) dispersion impellers.**Table 3. Power Constants for the Impellers**

impeller type	$K_p$	$N_p$
anchor	230	$f(Re)$
Rushton	75	5.00
Cowles	65	0.45
Deflo	65	0.60
Sevin	70	0.55
hybrid	70	0.50

in each experiment, it is typical to obtain such a consistency.<sup>17</sup> Although they have different geometries, the dispersion turbines do not exhibit significant differences in terms of their power consumption. Often operated in a turbulent regime with low-viscosity fluids,<sup>19</sup> from an energy perspective, the Cowles turbine is the most efficient.

In the case of a shear-thinning fluid obeying the power-law model, the viscosity decreases when the shear rate is increased. To evaluate the power consumption of such a fluid, the so-called process viscosity must be determined. Metzner and Otto<sup>20</sup> showed that the average shear rate around the impeller can be correlated with the rotational speed by means of the proportionality parameter  $K_s$ , which is a function of the impeller geometry

$$K_s = \gamma_a/N \quad (3)$$

Once this parameter is known, the characteristic power curve of each agitator ( $N_p$  vs  $Re$ ) using a shear-thinning fluid can be determined. In the present work, the approach used to determine the  $K_s$  value was that of

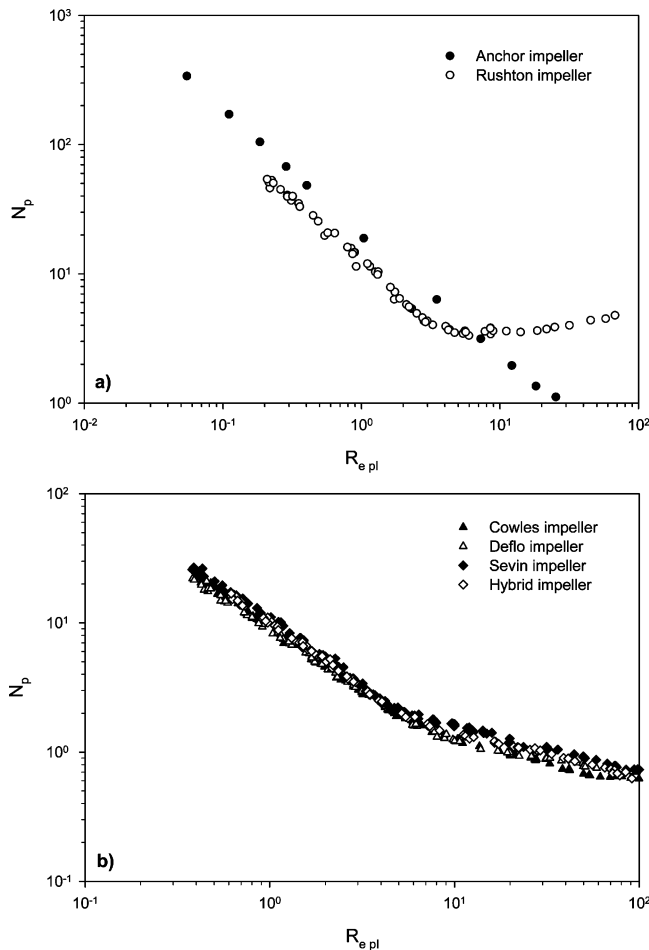


**Figure 5.** Non-Newtonian power curve for (a) Rushton and anchor impellers and (b) dispersion impellers.

Rieger and Novak,<sup>21</sup> in which a modified Reynolds number, often called the power-law Reynolds number,  $Re_{pl}$ , is used to draw the curve ( $N_p$  vs  $Re_{pl}$ )

$$Re_{pl} = \frac{\rho N^{2-n} D^2}{\kappa} \quad (4)$$

where  $k$  and  $n$  are the consistency index and the power-law index, respectively, of the fluid.

By plotting the corresponding power consumption curves for Newtonian and non-Newtonian fluids, the  $K_s$  value can be expressed in terms of their respective  $K_p$  values as follows

$$K_s = \left[ \frac{K_p(n)}{K_p} \right]^{1/n-1} \quad (5)$$

Figure 5 shows the characteristic power curves of all of the agitators investigated with the shear-thinning fluid. Because the Metzner and Otto concept<sup>20</sup> is valid for the laminar regime only, only the laminar parts of the curves are presented.

From Figure 5a and b, it is observed again that a constant slope equal to  $-1$  is obtained in the laminar regime, which is in good agreement with theory. Table 4 shows the corresponding  $K_p(n)$  values as well as the Metzner–Otto parameter  $K_s$  for all of the agitators with the shear-thinning fluid. The  $K_s$  value allows one to obtain a good indication of the shear stress in the vicinity of the blade using the Metzner and Otto

**Table 4.** Values of  $K_p(n)$  and  $K_s$  for Each Agitators

impeller type	$K_p(n)$	$K_s$
anchor	20.0	22
Rushton	12.5	10
Cowles	10.0	11
Deflo	10.0	11
Sevin	10.8	11
hybrid	10.0	12

method.<sup>20</sup> The  $K_s$  constants for the Rushton turbine and the anchor are in good agreement with the values reported elsewhere.<sup>17</sup>

In our work,  $K_s$  was found to be a constant that depends only on the system geometry. However, in many studies,  $K_s$  has been found to vary not only with geometrical parameters but also with the flow behavior index,  $n$ .<sup>22</sup> Here, we could not observe the influence of the shear-thinning index on the  $K_s$  values, because only two non-Newtonian fluids were considered.

**Coaxial Mixer.** In contrast to the power curve of a classical agitation system, the power curve of a coaxial mixer cannot be easily determined. In fact, in such a system, the choice of the characteristic diameter and speed required to calculate  $N_p$  and  $Re$  is ambiguous. According to our best knowledge, not many studies have tried to characterize the power consumption of such a system, except the few investigation mentioned in the preceding literature survey.

We analyzed the influence of the speed ratio ( $R_N = N_t/N_a$ ) on the power consumption of each agitator (central turbines and anchor). Figure 6 shows the characteristic power curve of the anchor for different

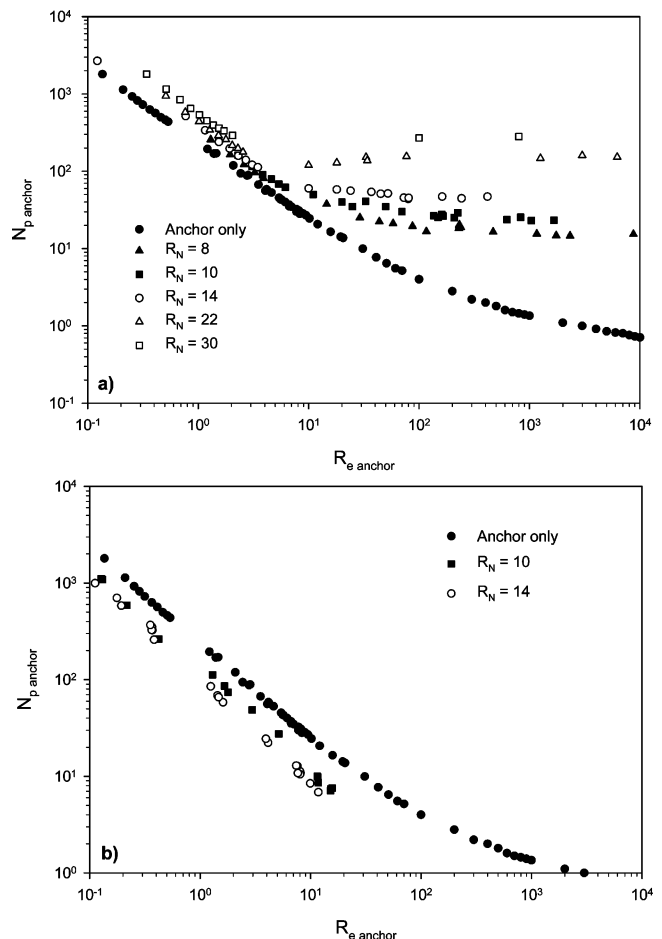


**Figure 6.** Power curve for the anchor as a function of the Rushton turbine speed: (a) counterrotating mode, (b) corotating mode.

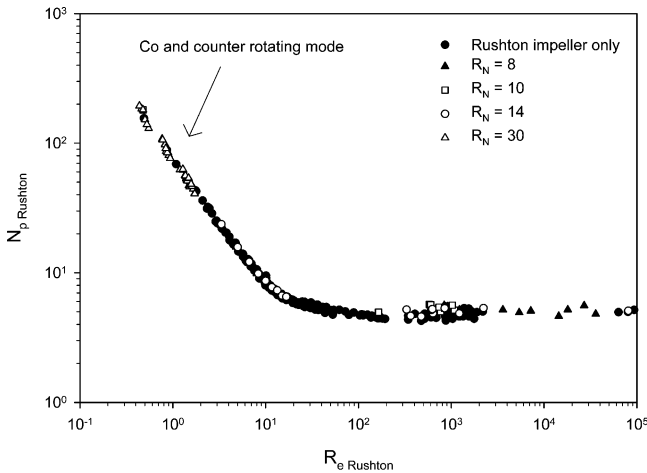


**Figure 7.** Power curve for the Rushton turbine as a function of the anchor speed.

speed ratios between the Rushton turbine and the anchor, in both counter- and corotating modes for a Newtonian fluid.

In both rotational modes, at very low  $R_e$  (laminar regime), the mixing theory (based on dimensional analysis) is satisfied as the power curves are parallel and their slope is  $-1$ . In counterrotating mode, the onset of the transition regime seems to be influenced by the speed ratio. The higher the speed ratio, the lower the value of the critical Reynolds number where the transition regime starts. For a speed ratio higher than 8, the turbulent regime is obtained for  $R_e$  values larger than 100. However, in corotating mode, we could not observe any influence of the speed ratio on the onset of the transition regime.

It can also be observed that the anchor power draw increases with the Rushton turbine in counterrotating mode and decreases in corotating mode. This can be explained by the addition or subtraction of the different pressure forces applied to the moving anchor. In counterrotating mode, the radial and tangential speed induced by the Rushton turbine causes an inverse repulsive force on the anchor blades, which increases the total power draw. In the reverse case, the turbine-induced flow drags the anchor in the flow direction, and as a consequence, a lower power draw is obtained. The same trends were observed for the dispersion turbines (not shown here).

We determined that, in the laminar and turbulent regimes, the variation of the total power constant ( $K_{p,anchor}$ ) and ( $N_{p,anchor}$ ) exhibits a polynomial dependence on the speed ratio (eqs 6 and 7)

$$K_{p,anchor}(R_N) = 13.16R_N^2 + 9.74R_N + 230 \quad 0 \leq R_N \leq 30 \quad (6)$$

$$N_{p,anchor}(R_N) = 0.62R_N^{2.77} \quad 0 \leq R_N \leq 30 \quad (7)$$

These two equations, in agreement with earlier studies,<sup>12,13</sup> allow for the estimation of the coaxial mixer (Rushton turbine/anchor) power draw for Newtonian fluids as a function of the speed ratio in counterrotating mode. However, no such a relation could be obtained in corotating mode.

Figures 7 and 8 show the characteristic power curves for the Rushton turbine and the Deflo turbine for different speed ratios in counter- and corotating modes.

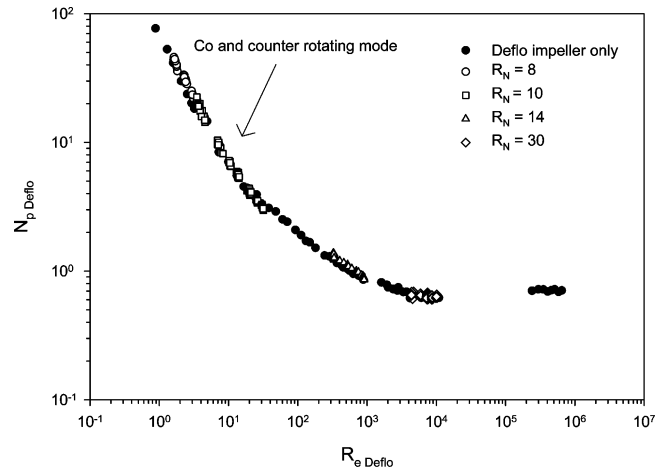


**Figure 8.** Power curve for the Deflo turbine as a function of the anchor speed.

In contrast to the anchor power consumption, the turbine power draw is not affected by the anchor speed. As Figures 7 and 8 show, a single characteristic power curve is obtained regardless the speed ratio. Similar results are obtained in the case of the dispersion turbines, which is in good agreement with the results reported by Foucault et al.<sup>15</sup> Taking into account the fact that the central agitator power number is independent of the speed ratio, the power drawn by the coaxial mixer can be correlated with the characteristic impeller diameter. The Reynolds number was then modified according to the rotation mode. Equations 8 and 9 express the Reynolds number used to determine the coaxial mixer power curve in Newtonian and non-Newtonian fluids

$$R_{e(\text{counterrotation})} = \frac{\rho(N_t + N_a)D_t^2}{\mu}, \quad R_{e(\text{corotation})} = \frac{\rho(N_t - N_a)D_t^2}{\mu} \quad (8)$$

$$R_{epl(\text{counterrotation})} = \frac{\rho(N_t + N_a)^{2-n}D_t^2}{\mu}, \quad R_{epl(\text{corotation})} = \frac{\rho(N_t - N_a)^{2-n}D_t^2}{k} \quad (9)$$

where  $N_t$  is the turbine speed,  $N_a$  is the anchor speed, and  $D_t$  is the characteristic diameter.

In counterrotating mode, the anchor speed is added to the speed of the central turbine. In corotating mode, the anchor speed is subtracted. As eqs 10 and 11 show, the same reasoning can be used to calculate the total power number of the system (impeller power + anchor power) in counterrotating and corotating modes

$$N_{p(\text{counterrotation})} = \frac{P_{tot}}{\rho(N_t + N_a)^3 D_t^5} \quad (10)$$

$$N_{p(\text{corotation})} = \frac{P_{tot}}{\rho(N_t - N_a)^3 D_t^5} \quad (11)$$

It should be noted that these correlations were experimentally determined and were found to be the best choice among several other possible definitions. Figure 9 shows the coaxial mixer power curve (Rushton

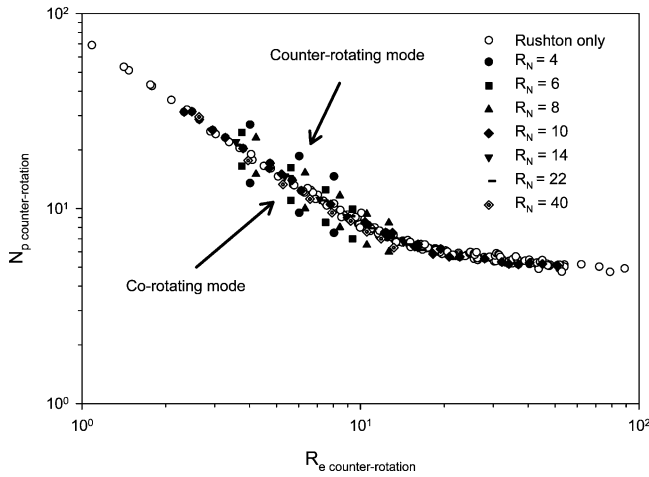


**Figure 9.** Power curves for the Rushton impeller in co- and counterrotating modes.

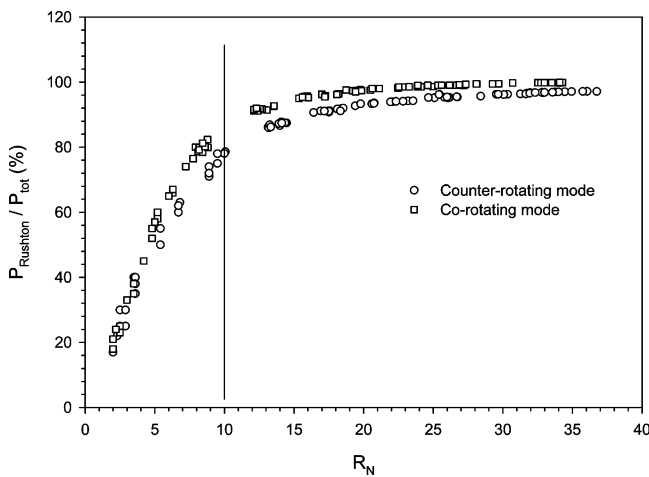


**Figure 10.** Relative power input of the Rushton agitator ( $P_{Rushton}/P_{tot}$ ) as a function of the speed ratio.

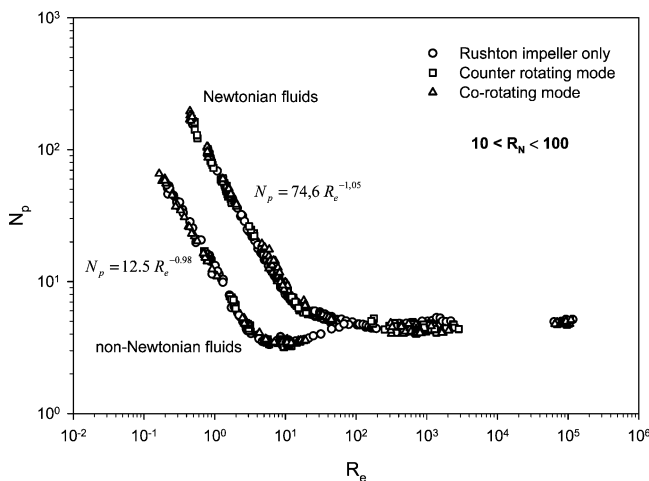


**Figure 11.** Power curve for Newtonian and shear-thinning fluids (Rushton turbine/anchor for  $R_N > 10$ ).

turbine/anchor) correlated with eqs 8–11 in counter-rotating and corotating modes. It must be mentioned that the new  $R_e$  and  $N_p$  correlations are available only for speed ratios higher than 10. Under this critical value of the speed ratio, the curve is shifted because the power drawn by the anchor is much higher than that drawn by the Rushton turbine. Figure 10 shows an example of the relative power input by the Rushton agitator

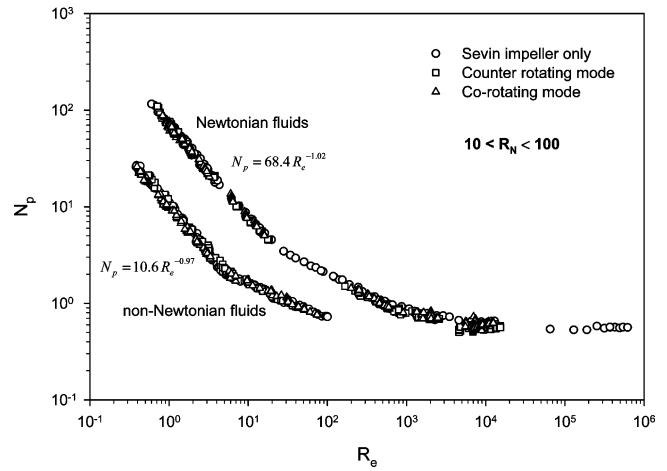


**Figure 12.** Power curve for Newtonian and shear-thinning fluids (Cowles turbine/anchor for  $R_N > 10$ ).

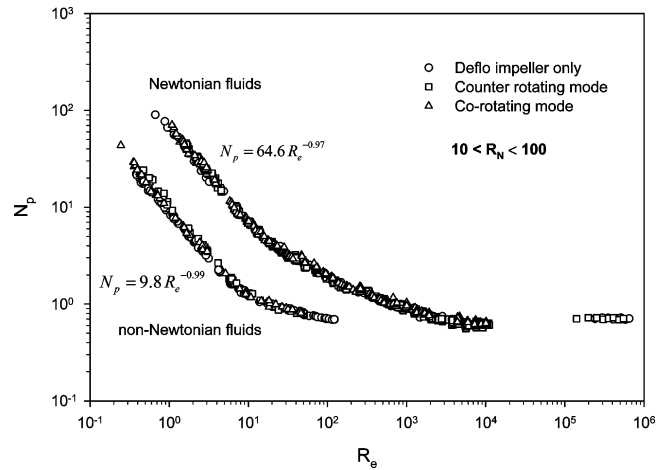


**Figure 13.** Power curve for Newtonian and shear-thinning fluids (Deflo turbine/anchor for  $R_N > 10$ ).

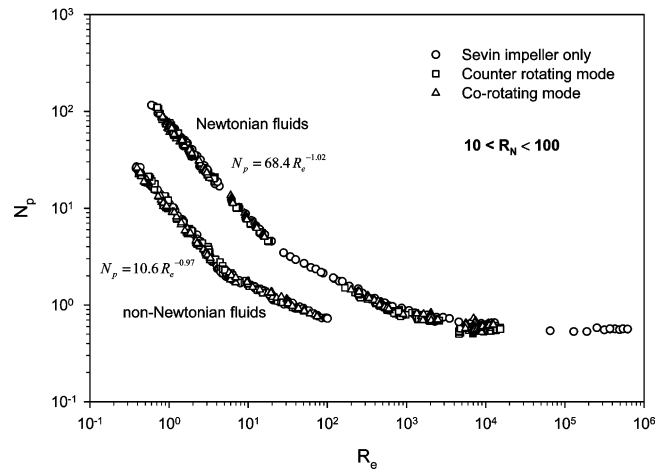


**Figure 14.** Power curve for Newtonian and shear-thinning fluids (Sevin turbine/anchor for  $R_N > 10$ ).

( $P_{Rushton}/P_{tot}$ ) in co- and counterrotating modes. The effect of the speed ratio on the distribution of the total power input between the Rushton and anchor impellers is remarkable. In co- and counterrotating modes, the relative power input of the Rushton impeller varies from 80% to 95% when the speed ratio is higher than 10.

Using these new  $R_e$  and  $N_p$  correlations, we are now able to determine the power curve of the coaxial mixer for speed ratios higher than 10. Figures 11–15 show

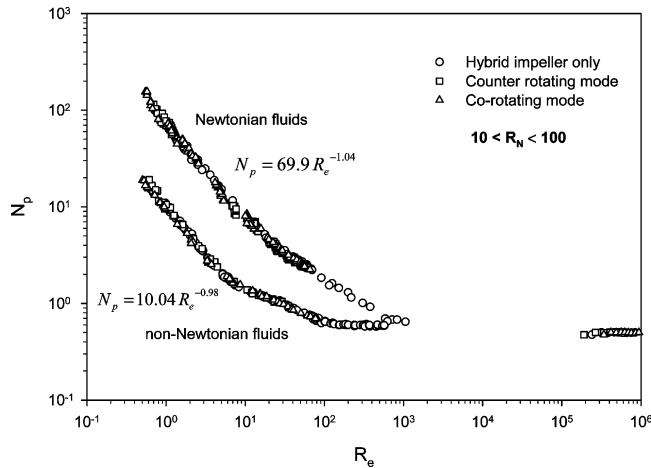


**Figure 15.** Power curve for Newtonian and shear-thinning fluids (hybrid turbine/anchor for  $R_N > 10$ ).

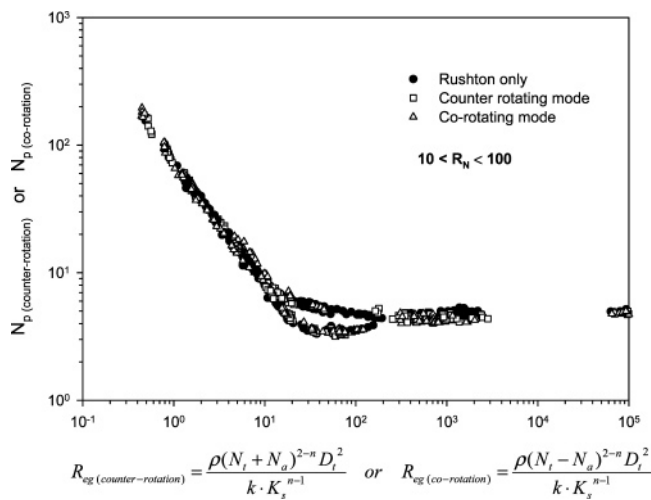


**Figure 16.** Power master curve for Newtonian and shear-thinning fluids based on the Metzner–Otto concept (Rushton anchor).

the power curves obtained by using eqs 8–11 for each impeller/anchor combination. In each case, the curves were determined for speed ratios from 10 to 100 with Newtonian and shear-thinning fluids. For  $R_N > 10$ , the modified correlations of  $R_e$  and  $N_p$  allow a single power curve to be obtained for the coaxial mixer operating in the three regimes.

According to the Metzner and Otto approach,<sup>20</sup> the constant  $K_s$  can be used to define the Reynolds number for shear-thinning fluids. In this work, the generalized Reynolds number in counter- and corotating modes was expressed as follows

$$R_{eg(\text{counterrotation})} = \frac{\rho(N_t + N_a)^{2-n} D_t^2}{k K_s^{n-1}} \quad (12a)$$

and

$$R_{eg(\text{corotation})} = \frac{\rho(N_t + N_a)^{2-n} D_t^2}{k K_s^{n-1}} \quad (12b)$$

The power master curve can then be plotted by means of the generalized Reynolds number (eqs 12) and the power number as expressed by eqs 10 and 11. Figures 16 and 17 show the resulting master curves for the

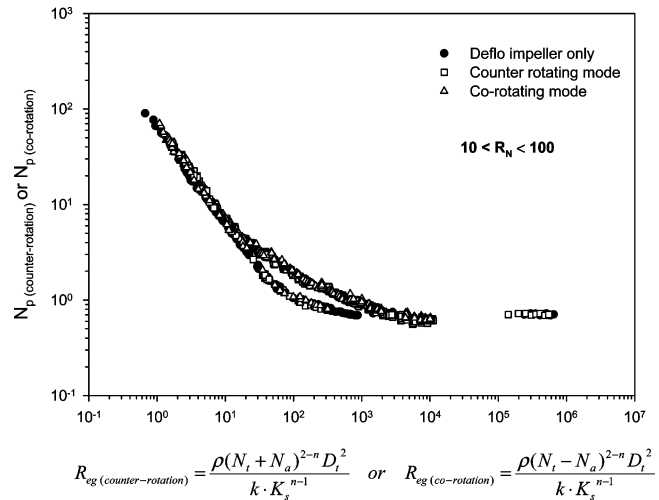


**Figure 17.** Power master curve for Newtonian and shear-thinning fluids based on the Metzner–Otto concept (Deflo impeller/anchor).

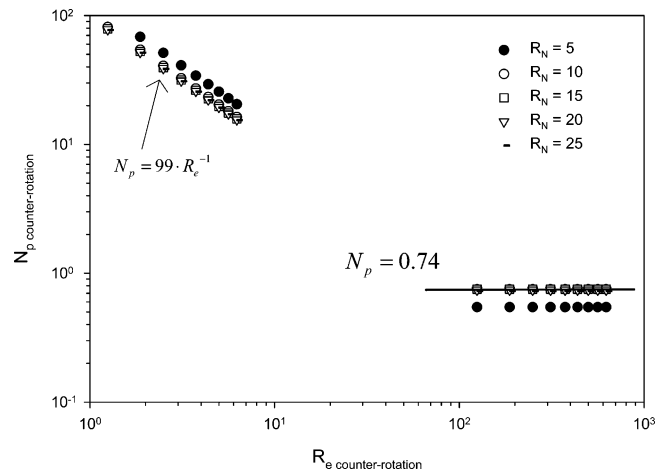


**Figure 18.** Power curve for Newtonian fluids in counterrotating mode based on the Tanguy and Thibault<sup>12</sup> data.

coaxial mixer with the Rushton turbine and with the Deflo turbine ( $10 < R_N < 100$ ).

These graphs allow for the determination of the power consumption of the coaxial mixer for speed ratios higher than 10 with Newtonian and shear-thinning fluids obeying the power-law model and for both counter- and corotating modes. The advantage of these correlations is that they can be applied to different coaxial mixer configurations. To validate this approach, the results obtained here were compared with those of Tanguy and Thibault<sup>12,13</sup> to determine the total power consumption in the laminar and turbulent regimes. In this case, it was assumed that the power consumption of the rods in their mixer was not affected by the anchor speed, so that the total power consumption for speed ratios between 5 and 25 could be obtained. In the laminar and turbulent regimes, the values of  $K_p = 99$  and  $N_p = 0.74$  for the fast shaft were used to determine the power of the mixers. Figure 18 shows the power curve of the coaxial mixer used by Tanguy and Thibault<sup>12,13</sup> as generated by our correlations in counterrotating mode. Similar trends are observed for a speed ratio higher than 10 in the laminar and turbulent regimes, or in other words, a unique master curve is obtained. For  $R_N = 5$ , the curve is shifted because the power drawn by the anchor is much higher.

## Conclusions

The objective of this study was to experimentally characterize the power drawn by a coaxial mixer consisting of a wall-scraping anchor and different dispersion impellers operating in co- and counterrotating modes in the case of Newtonian and shear-thinning fluids. It was demonstrated that, for all of the agitator combinations examined, the power consumption of the anchor increased significantly in counterrotating mode and decreased in corotating mode. On the other hand, no influence of the anchor was observed on the power dissipated by the dispersion impellers. Following the Metzner and Otto concept,<sup>20</sup> new correlations for  $N_p$  and  $R_{eg}$  were proposed to obtain a unique master curve for Newtonian and shear-thinning fluids. For speed ratios ( $R_N = N_t/N_a$ ) higher than 10, the coaxial power master curve was exactly the same as that of the turbine alone. For speed ratios smaller than 10, the new correlations proposed do not apply, and the mixer power curve is shifted from the master curve.

## Acknowledgment

The financial assistance of NSERC and Paprican is gratefully acknowledged.

## Nomenclature

$C_w$  = gap between the anchor and the wall, m  
 $C$  = clearance of the impeller off the tank, m  
 $D$  = impeller diameter, m  
 $D_a$  = anchor impeller diameter, m  
 $D_c$  = tank diameter, m  
 $D_t$  = turbine impeller diameter, m  
 $G'$  = storage modulus (Pa)  
 $G''$  = loss modulus (Pa)  
 $H_c$  = tank height, m  
 $H_l$  = liquid height, m  
 $k$  = consistency index,  $\text{Pa}\cdot\text{s}^n$   
 $K_p$  = power constant with Newtonian fluids  
 $K_p(n)$  = power constant with non-Newtonian fluids  
 $K_s$  = Metzner–Otto constant or shear constant  
 $L$  = impeller height, m  
 $n$  = shear-thinning index  
 $N$  = rotational speed, rps  
 $N_a$  = anchor rotational speed (low speed shaft), rps  
 $N_p$  = power number  
 $N_t$  = turbine rotational speed (high-speed shaft), rps  
 $P$  = power, w  
 $P_{tot}$  = total power of the system, w  
 $R_e$  = Reynolds number  
 $R_{eg}$  = generalized Reynolds number  
 $R_{epl}$  = power-law Reynolds number  
 $R_N$  = speed ratio ( $N_t/N_a$ )  
 $W_a$  = anchor blade thickness, m

## Greek Letters

$\dot{\gamma}$  = shear rate,  $\text{s}^{-1}$   
 $\dot{\gamma}_a$  = apparent shear rate,  $\text{s}^{-1}$   
 $\mu_a$  = apparent viscosity,  $\text{Pa}\cdot\text{s}$   
 $\rho$  = density,  $\text{kg}/\text{m}^3$

## Literature Cited

- Holland, F. A.; Chapman, F. S. *Liquid Mixing and Processing in Stirred Tanks*; Reinhold Publishing Co.: New York, 1966.
- Salomon, J.; Elson, T. P.; Nienow, A. W. Cavern Sizes in Agitated Fluids with a Yield Stress. *Chem. Eng. Commun.* **1981**, *11*, 143–164.

- Lamberto, D. J.; Alvarez, M. M.; Muzzio, F. J. Experimental and Computational Investigation of the Laminar Flow Structure in a Stirred Tank. *Chem. Eng. Sci.* **1999**, *54*, 919–942.

- Tanguy, P. A.; Brito-De La Fuente, E. Non-Newtonian mixing with helical ribbon impellers and planetary mixers. In *Advances in the Flow and Rheology of Non-Newtonian Fluids*; Rheology Series 8; Elsevier: New York, 1999; pp 301–359.

- Dubois, C.; Thibault, F.; Tanguy, P. A.; Ait-Kadi, A. Characterization of viscous mixing in a twin intermeshing conical helical mixer. *Inst. Chem. Eng. Symp. Ser.* **1996**, *140*, 249–258.

- Vanhove, D.; Biay, I. Characterization of counter-rotating agitation for a gel-preparation reactor. *Récents Progrès en Génie des Procédés (Etudes et Conception d'Équipements)* **1993**, *7* (30), 97–102.

- Tanguy, P. A.; Thibault, F.; Brito-De La Fuente, E.; Espinosa-Solares, T.; Tecante, A. Mixing performance induced by coaxial flat blade-helical ribbon impellers rotating at different speeds. *Chem. Eng. Sci.* **1997**, *52* (11), 1733–1741.

- Espinosa-Solares, T.; Brito-De La Fuente, E.; Tecante, A.; Tanguy, P. A. Power consumption of a dual turbine-helical ribbon impeller mixer in ungasged conditions. *Chem. Eng. J.* **1997**, *67* (3), 215–219.

- Espinosa-Solares, T.; Brito-De la Fuente, E.; Tecante, A.; Tanguy, P. A. Flow patterns in rheologically evolving model fluids produced by hybrid dual mixing systems. *Chem. Eng. Technol.* **2001**, *24* (9), 913–918.

- Espinosa-Solares, T.; Brito-De la Fuente, E.; Tecante, A.; Tanguy, P. A. Gas dispersion in rheologically evolving model fluids by hybrid dual mixing systems. *Chem. Eng. Technol.* **2002**, *25* (7), 723–727.

- Espinosa-Solares, T.; Brito-De La Fuente, E.; Tecante, A.; Medina-Torres, L.; Tanguy, P. A. Mixing time in rheologically evolving model fluids by hybrid dual mixing systems. *Chem. Eng. Res. Des.* **2002**, *80* (A8), 817–823.

- Tanguy, P. A.; Thibault, F. Power consumption in the turbulent regime for a coaxial mixer. *Can. J. Chem. Eng.* **2002**, *80* (4), 601–603.

- Thibault, F.; Tanguy, P. A. Power-draw analysis of coaxial mixer with Newtonian and non-Newtonian fluids in the laminar regime. *Chem. Eng. Sci.* **2002**, *57*, 3861–3872.

- Köhler, S.; Hemmerle, W. Analysis of the power characteristic of a coaxial agitator with varied diameter and speed ratio of inner and outer mixing device. In *Proceedings of the 11th European Conference on Mixing, Bamberg, Germany*; VDI-Gesellschaft Verfahrenstechnik und Chemieingenieurwesen (VDI-GVC): Berlin, 2003; pp 14–17.

- Foucault, S.; Ascanio, G.; Tanguy, P. A. Coaxial Mixer Hydrodynamics with Newtonian and non-Newtonian Fluids. *Chem. Eng. Technol.* **2004**, *27* (3), 324–329.

- Harnby, N.; Nienow, A. W.; Edwards, M. F. *Mixing in the Process Industries*, 2nd ed.; Butterworth-Heinemann: Woburn, MA, 1997.

- Nagata, S. *Mixing—Principles and Applications*; John Wiley & Sons: New York, 1975.

- Roustan, M. Agitation, Mélange, Caractéristiques des mobiles d'agitation. *Techniques de l'Ingénieur*; Vol. Génie des Procédés, Rubrique Formulation, 1999; Form. J3 802, 1–10 (available at www.techniques-ingenieur.fr).

- Furling, O.; Tanguy, P. A.; Henric, P.; Denoel, D.; Choplin, L. New dispersing turbines for the preparation of concentrated suspensions. *J. Chem. Eng. Jpn.* **2001**, *34* (5), 634–639.

- Metzner, A. B.; Otto, R. E. Agitation of Non-Newtonian Fluids. *AIChE J.* **1957**, *3* (1), 3–10.

- Rieger, F.; Novak, V. Power Consumption of Agitators in Highly Viscous Non-Newtonian Liquids. *Trans. Inst. Chem. Eng.* **1973**, *51*, 105–111.

- Shekhar, S. M.; Jayanti, S. Mixing of Power-Law Using Anchors: Metzner–Otto Concept Revisited. *AIChE J.* **2003**, *49* (1), 30–40.

Received for review April 28, 2004  
 Revised manuscript received June 14, 2004  
 Accepted June 17, 2004